



# Altered functional connectivity density in primary angle-closure glaucoma patients at resting-state

Linglong Chen<sup>1</sup>, Shenghong Li<sup>1</sup>, Fengqin Cai<sup>1</sup>, Lin Wu<sup>1</sup>, Honghan Gong<sup>1</sup>, Chonggang Pei<sup>2</sup>, Fuqing Zhou<sup>1,3</sup>, Xianjun Zeng<sup>1,3</sup>

<sup>1</sup>Department of Radiology, <sup>2</sup>Department of Ophthalmology, The First Affiliated Hospital, Nanchang University, Nanchang 330006, China; <sup>3</sup>Jiangxi Medical Imaging Research Institute, Nanchang 330006, China

*Correspondence to:* Xianjun Zeng. Department of Radiology, The First Affiliated Hospital of Nanchang University, Number 17, Yongwai Zheng Street, Donghu District, Nanchang 330006, China. Email: xianjun-zeng@126.com.

**Background:** Primary angle-closure glaucoma (PACG) is a neurodegenerative disease. Previous structural and functional studies of functional magnetic resonance imaging (fMRI) have demonstrated widespread dysfunction of spontaneous activity in the PACG brain. In this study, we applied a data-driven graph theory approach of functional connectivity density (FCD) mapping to investigate the altered local and global functional connectivity (FC) of the cortex in PACG.

**Methods:** Forty-five PACG patients (53.28±10.79 years, 17 males/28 females) and 46 well-matched healthy controls (HCs) (52.67±11.01 years, 18 males/28 females) received resting-state fMRI scans. All PACG patients finished complete ophthalmologic examinations, including retinal nerve fiber layer thickness (RNFLT), intraocular pressure (IOP), average cup to disc ratio (A-C/D), and vertical cup to disc ratio (V-C/D). We calculated the between-group FCD difference for short-range and long-range in each voxel. Then, we generated the intrinsic FC of the seed region with the whole brain. Finally, correlations were investigated between FCD value of the altered regions and clinical variables.

**Results:** PACG patients showed increased short-range FCD in the left inferior frontal gyrus (IFG)/insula/parahippocampal gyrus and right IFG/insula ( $P<0.05$ , corrected), compared with the HCs. Simultaneously, the decreased regions in short-range FCD map were the occipital/cuneus/precuneus/superior parietal/postcentral lobe ( $P<0.05$ , corrected). In the PACG groups, decreased long-range FCD was observed in the left middle frontal gyrus compared to the HC ( $P<0.05$ , corrected). RNFLT was positively correlated with decreased short-range FCD value of the occipital/cuneus/precuneus/superior parietal/postcentral lobes, and the A-C/D was negatively correlated with the increased short-range FCD value of the left IFG/insula/parahippocampal gyrus, and the right IFG/insula.

**Conclusions:** Our findings suggest that PACG can induce extensive brain dysfunction, and showed different spatial distribution in short- and long-range FCD.

**Keywords:** Primary angle-closure glaucoma (PACG); resting-state functional magnetic resonance imaging (fMRI); functional connectivity (FC); functional connectivity density mapping (FCD mapping); visual pathway

Submitted Nov 26, 2018. Accepted for publication Apr 22, 2019.

doi: 10.21037/qims.2019.04.13

**View this article at:** <http://dx.doi.org/10.21037/qims.2019.04.13>

## Introduction

Glaucoma is the second leading cause of blindness in the world. Glaucoma is characterized by a progressive apoptosis of retinal ganglion cells (RGCs), the clinical manifestation of visual-field loss, and cupping of the optic nerve (1). In Asia, primary angle-closure glaucoma (PACG) is more common than primary open angle glaucoma (POAG). The pathological increase of intraocular pressure (IOP) is a principal risk factor for glaucoma, causing optic neuropathy and eventually RGC death (2). However, extensive neuroimaging studies, including those using functional magnetic resonance imaging (fMRI), have confirmed that the damage is not only limited to the anterior visual pathway but occurs in the cerebral cortex as well. Misfolded protein deposition, a key feature of neurodegenerative diseases, was found in the optic nerve and the visual cortex of glaucoma patients (3-6). Functional MRI at resting-state has been widely used to demonstrate the problem structurally and functionally (6-9), and widespread dysfunction of spontaneous activity has also been previously indicated (10-12).

However, more researchers have focused on POAG rather than PACG, and there have been no advanced studies concerning the global functional changes of PACG patients. Therefore, we chose a data-driven graph theory approach of functional connectivity density (FCD) mapping (13) to obtain intraregional and interregional spontaneous neuronal activity and connectivity [compared with regional homogeneity (ReHo) (14)], without any prior hypothesis [compared with hypothesis-driven resting-state functional connectivity (rsFC) analysis (15)]. This approach measures local and global significant functional connections of voxels over the whole brain, is suitable for investigating altered cortical functional connectivity (FC) of PACG, and provides complementary information for more targeted analysis. Previous studies have revealed that changes in FC are closely associated with the spontaneous release of synaptic neurotransmitters (16). Therefore, any abnormality in neural activity, such as apoptosis, and developmental, plastic, and degenerative mechanisms, would lead to a change of FCD. The approach of FCD was used to investigate the neural mechanisms of Parkinson's disease (17), and it may be suitable for investigating the different disorders across the brain when PACG occurs.

In our study, FCD mapping was applied to explore changes of intraregional and interregional FCD in PACG patients during the resting state. The main purposes of

this study were (I) to identify short- and long-range FCD abnormalities of PACG in resting-state based on the certain correlation rate, and (II) to relate the alterations of FC to clinical data by analyzing the correlation between clinical parameters and the significantly changed regions.

## Methods

### Subjects

Fifty pre-PACG patients ( $53.28 \pm 10.79$  years, 17 males/28 females) and 46 healthy controls (HCs) ( $53.28 \pm 10.79$  years, 18 males/28 females) were recruited from the Department of Ophthalmology of the First Affiliated Hospital, Nanchang University, China, in the period between 2013 October and 2017 October. All patients were included according to the following criteria: (I) pathologically increasing IOP  $>21$  mmHg; (II) cup-to-disc ratio (CDR) higher than 0.6 measured as revealed by optometry; (III) a shallow anterior chamber together with glaucoma-like visual-field loss, such as tubular vision and nasal hemianopia. Five patients were excluded due to having another kind of glaucoma, incomplete clinical or fMRI information, a history of psychotropic drug use, or had received previous surgical treatment. Forty-six age-matched HCs were recruited at the same time. All the HCs complied with the following standards: (I) no history of intraocular or intracranial diseases, and (II) normal visual acuity (VA) in both eyes. The clinical statistics of 45 PACG patients were collected by two experienced ophthalmologists: the IOP was measured using a tonometer, the retinal nerve fiber layer thickness (RNFLT), average cup-to-disc ratio (A-C/D), and vertical cup-to-disc ratio (V-C/D) were evaluated with the optical coherence tomography (Cirrus HD-OCT), and visual acuity (VA) was measured with the Peripheral Vision Test (Humphrey Field Analyzer, Humphrey HFA II-i). Detailed demographics of participants and clinical data are shown in *Table 1*.

This study complied with the Declaration of Helsinki, and the Human Research Ethics Committee of the First Affiliated Hospital of Nanchang University approved the study protocol. Written informed consent was obtained from each participant prior to the study.

### MRI data acquisition

All subjects were scanned by the same Siemens Trio 3.0 T scanner, with an 8-channel phased-array head coil, in the

**Table 1** General clinical information for primary angle-closure glaucoma (PACG) patients and normal controls (HCs)

Condition	PACG	HCs	P value
Mean age (years)	53.28±10.79	52.67±11.01	>0.99
Gender (male/female)	17/28	18/28	>0.99
Handedness (right/left)	45/0	46/0	>0.99
Mean disease duration (days) (range)	2–2,920	–	N/A
IOP (mmHg)	28.37±9.54	–	N/A
RNFLT ( $\mu\text{m}$ )	83.75±20.95	–	N/A
A-C/D	0.63±0.20	–	N/A
V-C/D	0.51±0.31	–	N/A
Mean VA (range)	0.52±0.29	–	N/A
Head motion	0.050±0.015	0.041±0.016	0.55

IOP, RNFLT, A-C/D, V-C/D, and VA are presented as mean binocular values. IOP, intraocular pressure; RNFLT, retinal nerve fiber layer thickness; A-C/D, average cup-to-disc ratio; V-C/D, vertical cup-to-disc ratio; VA, visual acuity; N/A, not applicable.

First Affiliated Hospital of Nanchang University, China. Each subject was comfortably kept in the supine position by a belt and foam pads during the 8-minute resting state fMRI (rs-fMRI) scanning, while staying awake, and keeping the head in a neutral position with eyes closed. A gradient-echo echo-planer imaging (EPI) sequence of 240 volumes was used for rs-fMRI data acquisition in an ascending (1, 3, 5...29; 2, 4, 6...30) interleaved order using the following parameters: repetition time (TR)/echo time (TE) = 2,000/40 ms, flip angle = 90°, field of view (FOV) = 240 mm × 240 mm, slice thickness/gap = 4.0/1 mm, inplane resolution = 64×64, 30 axial slices. Then, a T1-weighted 3D magnetization-prepared rapid gradient-echo (MP-RAGE) sequence was used to collect the high-resolution brain structural images using the following protocols: TR/TE = 1,900 ms/2.26 ms, matrix = 240×256, FOV = 215 mm × 230 mm, thickness = 1.0 mm, 176 sagittal slices without a slice gap, scanning time = 3 minutes.

### fMRI data preprocessing

We utilized Data Processing and Analysis of Brain Imaging (DPABI v2.1) (<http://www.rfmri.org/dpabi>) toolbox in Matlab (2014a, Math Works Inc., Natick, MA, USA) working platform for fMRI data preprocessing. The first ten volumes of each data set were discarded to avoid magnetization instability. The remaining 230 volumes were manipulated with the procedure of slice timing correlation and then realigned to the first volume to correct for head

motion. Realigning of resultant images were done following a criterion of head motion within 3 mm translations and 3° rotations. The Friston 24-parameter model was used to regress out head motion effects from the realigned data. We subsequently used the mean frame-wise displacement (FD) as a measure of the micro-head motion of each subject, by considering measures of voxel-wise differences in motion in its derivation. Subjects were excluded if their FD exceeded 0.3. Afterward, the realigned functional data were co-registered based on high-resolution T1-weighted structural images. The image data were then normalized to the standard Montreal Neurological Institute (MNI) space and resampled to a voxel size of 3×3×3 mm<sup>3</sup>, to regress out the nuisance variables. Finally, as frequencies under 0.01 Hz lead to low-frequency drifts, and those exceeding 0.08 Hz may indicate high-frequency physiological noise, band-pass filtering (0.01–0.08 Hz) was performed.

### Resting-state FCD calculation

FCD calculation was operated on a Graph-theoretical Network Analysis Toolkit (GRETNA v2.0.0) (<http://www.nitrc.org/projects/gretna/>) in Matlab platform based on the theory of Tomasi and Volkow (18,19). The correlation coefficient threshold ( $T_c$ ) was set to 0.3, as a higher  $T_c$  can lead to a higher false positive rate and more calculation time, while a lower  $T_c$  can reduce dynamic range and lower sensitivity. The rate ( $r$ ) of the correlation coefficient between a certain voxel and every other voxel over the

whole brain range was calculated; these two voxels were considered to be relative if  $r > 0.3$ . The threshold of the signal-to-noise ratio (SNR) was set to 0.5. The calculation results of every certain vowel made up global FCD, which means the function connection density distribution of the whole brain. According to He (20), we preferred to consider a given anatomical distance of 75 mm to be a long-range connection, which means an intra-regional effective functional connection. Then, the difference between the global FCD and long-range FCD was the value of the short-range. The long- and short-range FCD maps were normalized for the result to be in a normal distribution. Finally, the normalized FCD data were spatially smoothed with a Gaussian kernel of  $6 \times 6 \times 6 \text{ mm}^3$  depending on the full width at half maximum (FWHM), in order to increase the SNR and eliminate artifacts.

### Statistical analysis for FCD

First, the spatial distribution of mean short- and long-range FCD of PACG and HC was calculated. Then, we performed general linear model (GLM) analysis for between-group FCD comparisons using statistical parametric mapping (SPM8, <http://www.fil.ion.ucl.ac.uk/spm/software/spm8/>), while age, gender, and averaged FD were included as nuisance covariates. Two tailored Gaussian random field (GRF) corrections were used to reduce the false positive rate, with a threshold of voxel P value  $< 0.01$ , and a cluster P value  $< 0.05$ . The effect size (ES) was further estimated by Cohen's  $d$  (21) to determine the significant differences between groups of mean short- and long-range FCD in clusters.

### Region-of-interest-based FC calculation and statistical analysis

Seed-based FC analysis was performed on the region of interest (ROI) that showed significant differences between PACG and HC in the long-range FCD to investigate the altered FC of ROI and the whole brain. For each subject, the mean time courses of the ROI were extracted from all of the voxels in the ROI using DPABI (<http://rfmri.org/DPARF/>), while Pearson correlation coefficients of the mean time courses were calculated between pairwise ROIs for each subject. The resulting  $r$  values were converted to  $z$  values according to Fisher's  $r$ -to- $z$  transformation for further statistical analysis in order to obey a normal distribution. First, we used the FC for between-group comparison only

if the FC extracted from the ROIs between PACG patients and HCs were statistically significant within each group after a random effect one-sample  $t$ -test in SPM8. Next, the ROIs'  $z$ -values of the PACG and HC groups were evaluated by a GLM analysis in SPM8 after controlling for age and gender with the family-wise error (FWE) correction ( $P < 0.05$ , a cluster size of  $> 100$  voxels). The effect size (ES) was also estimated by Cohen's  $d$  (21) to determine the significant differences between groups. Finally, we assessed the correlations between values of altered long- and short-range FCD and ROI-based rsFC in PACG with clinical data by partial correlation analysis.

## Results

### Demographic and clinical data

Table 1 shows that the mean age of PACG patients was  $53.28 \pm 10.79$  years old, and the disease duration ranged from 2 days to 2,920 days. There were no significant differences between PACG patients and HCs in age, gender, or handedness.

### Spatial distribution of FCD

The spatial distribution maps of the short- and long-range FCD in the PACG patients and HCs are all shown in Figure 1. The short-range FCD hub regions showed similar spatial distributions in PACG patients and HCs. There are both wide distributions of long-range FCD and short-range FCD in the temporal/parietal/limbic lobe/cuneus. Additionally, the short-range FCD was observed to be higher in the precuneus/cingulate, while the long-range FCD was higher in the postcentral/precentral/medial frontal gyrus.

### Group differences in FCD and rsFC

The between-group comparison was computed to reveal differences in long-range FCD and short-range FCD (Table 2, Figure 2). Compared with the HCs, the relatively increased regions in the short-range FCD map were the left inferior frontal gyrus (IFG)/insula/parahippocampal gyrus and the right IFG/insula. Meanwhile, the relatively decreased regions in the short-range FCD map were the occipital/cuneus/precuneus/superior parietal/postcentral lobe. In the PACG groups, when compared to the HCs, a relatively decreased long-range FCD was observed in the middle frontal gyrus on the left hemisphere.

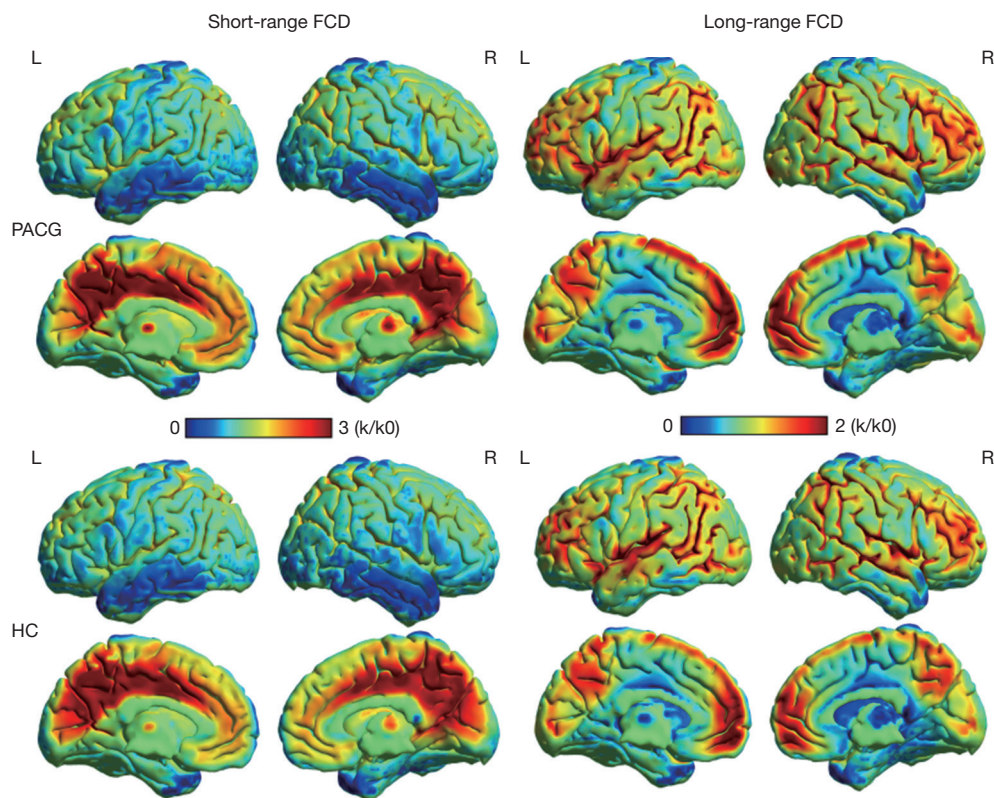


**Figure 1** Spatial distribution of short- and long-range FCD in the PACG and the HC groups, visualized with the BrainNet Viewer (<http://www.nitrc.org/projects/bnv/>). L, left; R, right; FCD, functional connectivity density; PACG, primary angle-closure glaucoma; HC, normal control;  $k/k_0$ , the normalized FCD.

### *Alteration in FC based on seed-region*

The region of the middle frontal gyrus which showed altered long-range FCD was defined as an ROI. The rsFC pattern of the middle frontal gyrus showed a significant group difference (Figure 3). Table 3 and Figure 4 show that in the between-group results of FC, there was significantly reduced FC between the middle frontal gyrus and the lingual/parahippocampal gyrus in PACG subjects.

### *Correlations between clinical data and short- and long-range FCD*

The correlation between the FCD value and rsFC was analyzed using the clinical data of the patients, the results of which are summarized in Figure 5. The decreased short-range FCD value of the occipital/cuneus/precuneus/superior parietal/postcentral lobe is positively correlated with RNFLT ( $r=0.302$ ,  $P<0.05$ ). The increased short-range FCD value of the right IFG/insula ( $r=-0.355$ ,  $P<0.05$ )

and the left IFG/insula/parahippocampal gyrus ( $r=-0.308$ ,  $P<0.05$ ) is negatively correlated with A-C/D. However, no significant relationship was found between V-C/D, IOP, or VA with the FCD value any of the altered regions.

### **Discussion**

Our primary finding is the different spatial distribution of changed long- and short-range FCD in visual and other regions by resting-state fMRI in PACG patients.

In our current study, we noticed a decreased short-range FCD in the wide areas of the visual cortex [occipital lobe (mainly in BA18/19), cuneus] and visual-associated regions (superior parietal lobe, postcentral lobe, and precuneus). BA18/19 is referred to as the higher visual cortex and receives information from the primary visual cortex. Chen *et al.* (22) found that both PACG patients had decreased regional spontaneous brain activity in the visual cortex. Previous studies found decreased cortical

**Table 2** Differences in the short-range FCD, long-range FCD, and gray matter volume between the PACG and HC groups

Brain regions	Cluster size (voxels)	BA	MNI coordinates			Peak T values	ES
			x	y	z		
<b>Increased short-range FCD</b>							
Left PHG/INS/IFG	428	30/47/34	-27	9	-21	4.29	-0.34
Right INS/IFG	441	44/45/13	48	18	6	4.80	0.43
<b>Decreased short-range FCD</b>							
Occipital/cuneus/preCUN/SPL/PCL	1,480	18/19/7	21	-90	18	-5.38	0.51
<b>Decreased long-range FCD</b>							
Left MFG	155	10	-30	39	27	-4.86	-0.35

Negative T value means the resting-state FCD in PACG is smaller than HC. Positive ES means the resting-state FCD in HC is larger than PACG. FCD, functional connectivity density; PACG, primary angle-closure glaucoma; HC, healthy control; BA, Brodmann area; MNI, Montreal Neurological Institute; ES, effect size; IFG, inferior frontal gyrus; PHG, parahippocampal gyrus; INS, insula; preCUN, precuneus; SPL, superior parietal lobe; PCL, Postcentral Lobe; MFG, middle frontal gyrus.

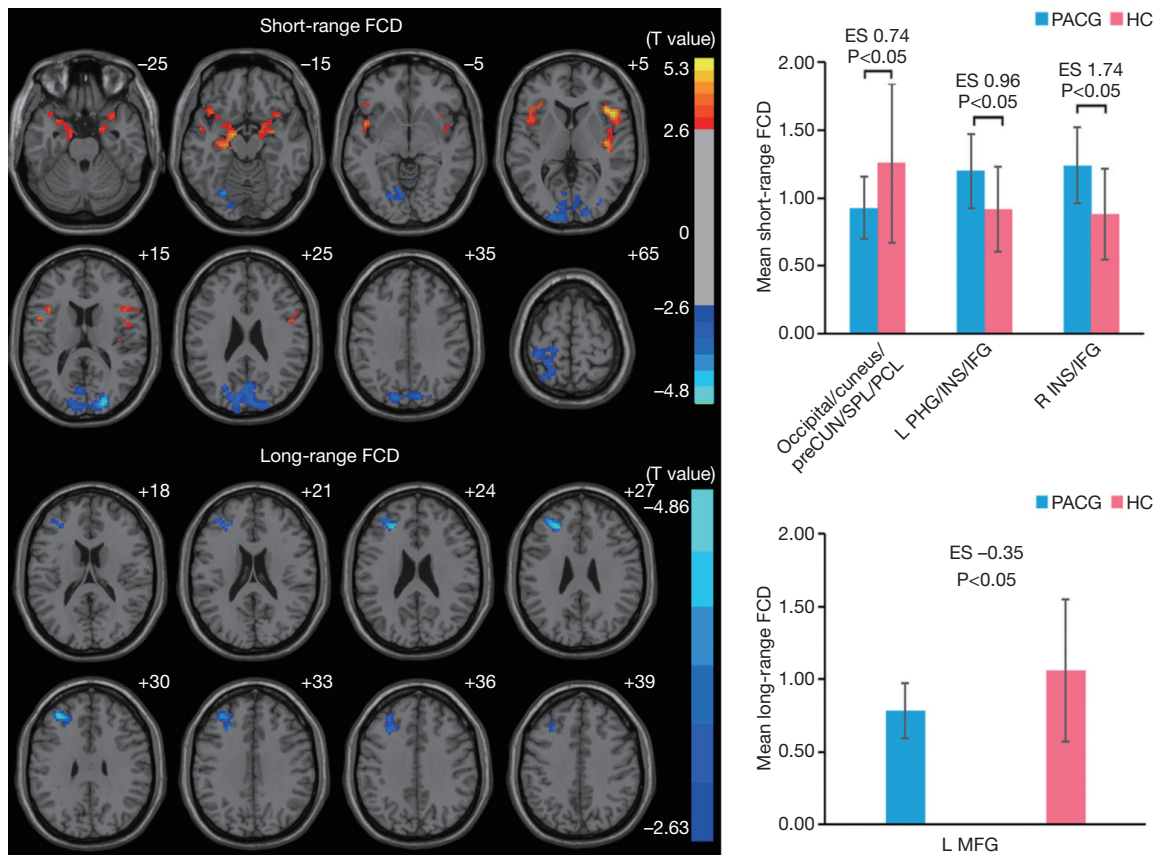


**Figure 2** Brain regions with significant changes in short- or long-range FCD in the PACG (voxel P value <0.01, cluster P value <0.05, corrected), visualized with the DPABI slice viewer (<http://rfmri.org/dpabi>). Significant group differences in the mean strength of the short- (above) and long-range (below) FCD in the above regions ( $P < 0.05$ ). The error bars are standard errors of the mean. FCD, functional connectivity density; PACG, primary angle-closure glaucoma; HC, healthy control; IFG, inferior frontal gyrus; PHG, parahippocampal gyrus; INS, insula; preCUN, precuneus; SPL, superior parietal lobe; PCL, postcentral lobe; MFG, middle frontal gyrus; R, right; L, left; ES, effect size.

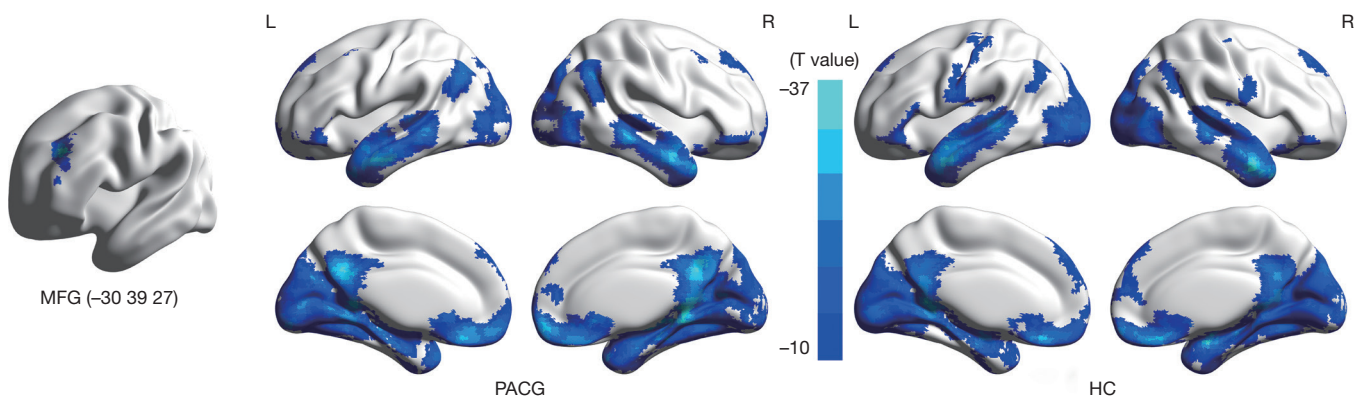


**Figure 3** Brain regions showed significant alteration ( $P < 0.05$ , corrected) in rsFC patterns with the left middle frontal gyrus between the PACG and the HC groups, visualized with the BrainNet viewer. rsFC, resting-state functional connectivity; PACG, primary angle-closure glaucoma; HC, healthy control; MFG, middle frontal gyrus.

**Table 3** rsFC differences between the PACG and HC groups

Functional connectivity	Cluster size (voxels)	BA	MNI coordinates			Peak T values	ES
			x	y	z		
Seed: L MFG							
Right PHG/Lingual	341	19/30	21	-21	-12	-4.6442	-0.28

rsFC, resting-state functional connectivity; PACG, primary angle-closure glaucoma; HC, healthy control; BA, Brodmann's area; MNI, Montreal Neurological Institute; ES, effect size; MFG, middle frontal gyrus; PHG, parahippocampal gyrus.

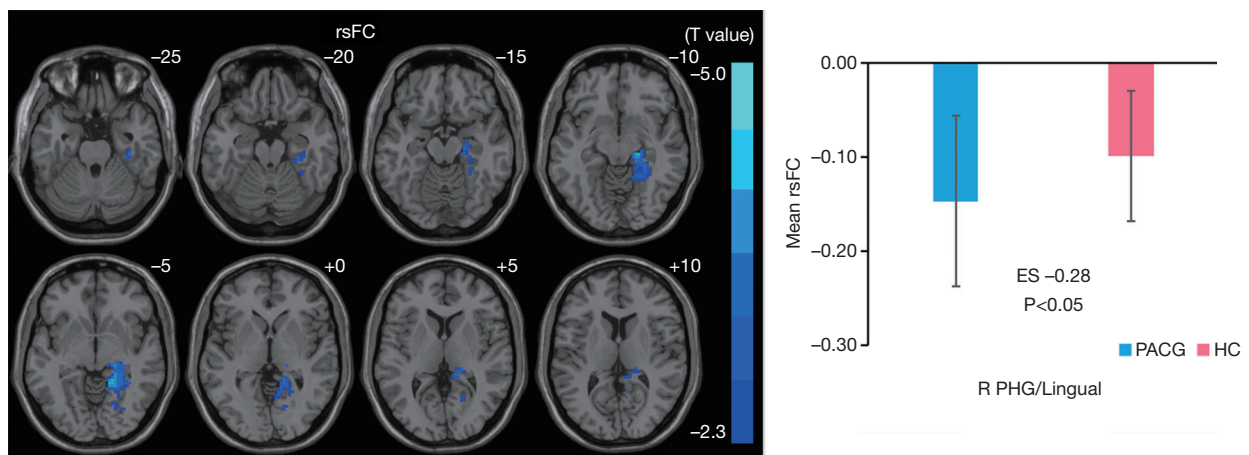


**Figure 4** Brain regions with significant changes in rsFC with the right middle frontal gyrus in the PACG (voxel  $P$  value  $< 0.01$ , cluster  $P$  value  $< 0.05$ , corrected), visualized with the DPABI slice viewer (<http://rfmri.org/dpabi>). Significant group differences in the mean strength of rsFC in the above regions ( $P < 0.05$ ). The error bars are standard errors of the mean. rsFC, resting-state functional connectivity; PACG, primary angle-closure glaucoma; HC, healthy control; PHG, parahippocampal gyrus; ES, effect size.

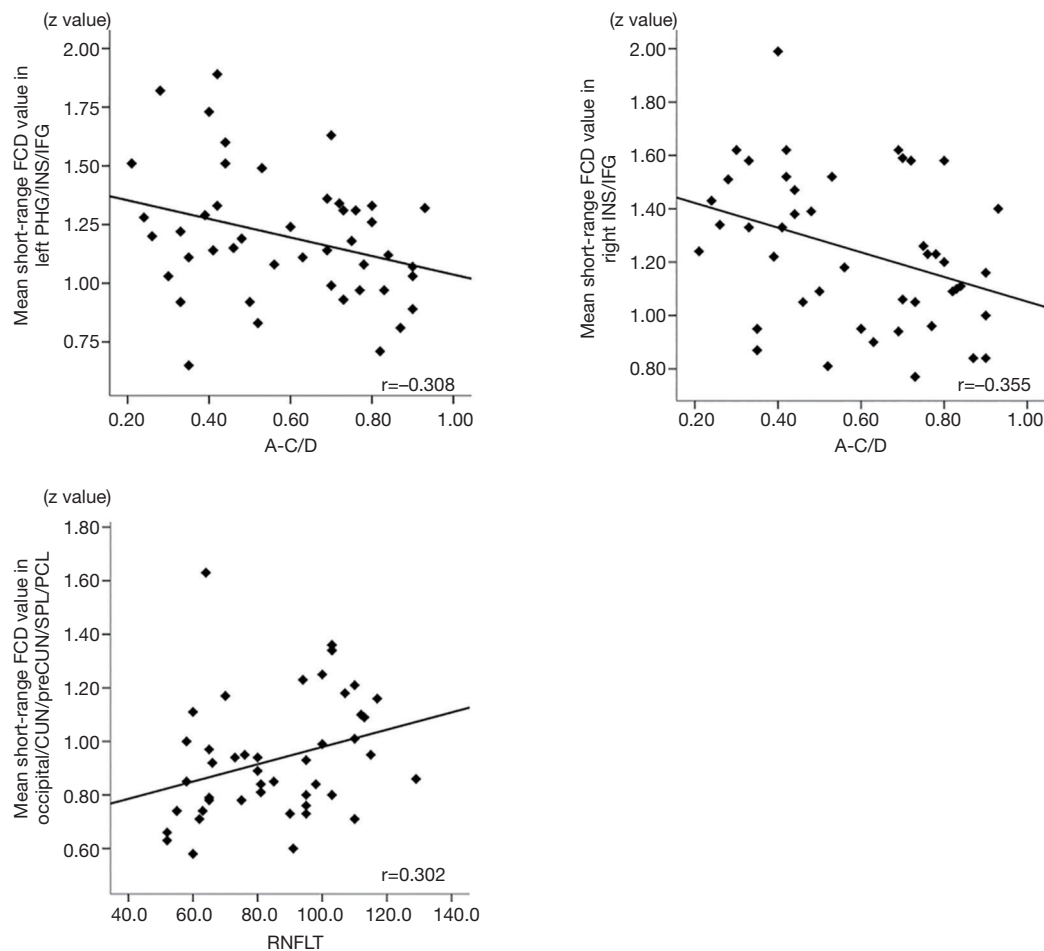


**Figure 5** Relationships between clinical indices and short-range FCD value in PACG patients. The decreased short-range FCD value of occipital/CUN/preCUN/SPL/PCL is positively correlated with retina nerve fiber layer thickness (RNFLT) ( $r=0.302$ ,  $P<0.05$ ). The increased short-range FCD value of the right INS/IFG ( $r=-0.355$ ,  $P<0.05$ ) and left PHG/INS/IFG ( $r=-0.308$ ,  $P<0.05$ ) is negatively correlated with A-C/D. FCD, functional connectivity density; PACG, primary angle-closure glaucoma; HC, healthy control; IFG, inferior frontal gyrus; PHG, parahippocampal gyrus; INS, insula; CUN, cuneus; preCUN, precuneus; SPL, superior parietal lobe; PCL, postcentral lobe; RNFLT, retinal nerve fiber layer thickness; A-C/D, average cup-to-disc ratio.

gray matter density (23) and progressive thinning of the visual cortex (24), which might be an anatomical substrate of the functional alteration. Disrupted regional metabolism may account for the decreased visual function because of decreased cerebral blood flow and the deposition of CHO-containing compounds (25). Moreover, research in other ophthalmic diseases of congenital or acquired defects, such as blind and anisometropic amblyopia, indicated varying degrees of lower short-range FCD value in the visual cortex. Corresponding to the above functional and structural findings, our result of a decreased short-range FCD confirms the disturbing of regional spontaneous activity in

the visual cortex. As a kind of neurodegenerative disease, glaucoma shares several biological features with Alzheimer's disease (AD) and Parkinson's disease (PD), such as a strong age-related incidence, the death of ganglion cells, and mechanisms of cell injury (3). Oxidative stress directly leads to the reduction of the synapse which manifests as a decreased FCD value.

According to our results, PACG showed a decreased short-range FCD in the postcentral lobe and the superior parietal lobe, which are involved in the dorsal "how" visual pathway crucial in spatial information processing. The postcentral lobe is a part of the dorsal visual pathway,

and the superior parietal lobe is structurally close to this pathway. The visual context information is transited to the superior parietal cortex for spatial processing, especially the right superior parietal lobe (26). Moreover, recent rs-fMR studies have found functional disruption in the postcentral lobe and the superior parietal lobe in PACG individuals, and a decreased FC was found between these regions of the visual cortex (8,27). In our result, we found that the regions with reduced short-range FCD involved the dorsal visual pathway more than the ventral visual pathway. Compared with our team's previous studies (10,11), the changes of the two visual pathways were not exactly the same after glaucoma occurrence, which may indicate the differentially impaired consolidation of the visual network.

Similar reductions of short-range FCD were also found in the precuneus and cuneus, which are also associated with visuospatial imagery such as detail selection in images (28). As an important node of the default mode network, the precuneus has the highest short-range FCD value in healthy subjects (17,29) and is more susceptible to the oxidative stress injury in neurodegenerative disease (30). The reduced short-range FCD of the precuneus and cuneus has been found in high myopia patients (31), while POAG has been associated with decreased regional homogeneity (7) and increased gray matter volume of the bilateral precuneus (32); the precuneus is also susceptible to visual impairment. Our results from these visual-associated regions may help us to understand the secondary impairment of visuospatial information processing.

The decreased short-range FCD value is positively correlated with the RNFLT of PACG, which verifies our previous conclusion that the dysfunction of the visual and visual-associated cortex may share a similar neuroinflammatory mechanism with the retina.

The regions of hyperactivity are involved in the visual-associated regions [the left parahippocampal gyrus (PHG)] and nonvisual regions (the bilateral insula and IFG). The PHG plays a causal role in the perception of visual scenes in the limbic system (21), given that PHG cells turn out to be sensitive and respond more quickly to visual stimuli than other nonvisual cells (21,31,33). In short, we speculate increased FCD may represent a compensatory enhancement of visual function as the PHG becomes more active when the visual deficit occurs. Second, increased long-range spontaneous activity was observed in the bilateral IFG. The left IFG (Broca's area) is a processing center for various language tasks for the most right-handed patients, and poor speech perception and visual speed discrimination of POAG

has been previously reported (34). Moreover, compared with the increased FC between the visual cortex and the left IFG/insula lobe found previously by our team (10), the hyperactivity of the IFG may indicate a compensatory activation.

In our findings, increased short-range FCD was found in the insula, the key node of the salience network (SN), which shows sensitivity to salient stimuli. Notably, the unhealthy coupling between the SN and the default-mode network (DMN) was found when degenerative diseases like PD occurred even at a very early stage (35). Apart from the DMN and SN, in our results, separated changes of the frontal lobe (stress and decision-making), precuneus [anxiety (36)] and the insula [depression (37)] may remain as unhealthy cognitive conditions of patients (38,39). Acute clinical symptoms can easily trigger patients' emotional reaction, and increased IOP was thought to be a triggering factor in the degeneration of the visual pathway. Thus, there remains an open question of whether the disorder of the cortex leads to psychological symptoms or whether the clinical symptoms directly result in these psychological symptoms, ultimately causing brain change.

The increased short-range FCD value was negatively correlated with the A C/D which was itself found to be positively correlated with the incidence of glaucoma and the damage of the anterior optic pathway (40). Our result provides the evidence for functional plasticity of the visual-associated regions or compensatory action of the other regions.

The long-range FCD referred to a relatively remote functional connection. Decreased long-range FCD was observed outside the visual cortex, principally involving the left middle frontal lobe (MFL). In a study by Li *et al.*, altered ALFF was also found in the right MFL. These results confirm the presence of disordered spontaneous activity of the MFL. As part of the working memory network, the frontal lobe also plays a significant role in cognitive control, be it visual or auditory, such as object-location memory encoding (41). Furthermore, decreased FC of PHG/lingual gyrus with MFL was found, indicating the decreased remote connection between them. The lingual gyrus is known as a stable region of the ventral stream, being in charge of an analysis of logical conditions and encoding visual memories (42), and joins the PHG which lies in front of the brain. In Dai *et al.*'s study, decreased negative FC were found between BA17 and the MFL in POAG (27). PACG patients suffer from abnormal visual input, which may bring about a series of cognitive defects, whether directly or indirectly associated with the

sense of vision. The hyperextension of MFL may be related to the decreased spontaneous activity of these two visual-associated regions.

### Strength and limitation

Because of the widespread progressive degeneration and correlation of brain regions, the use of FCD mapping to reveal the disorder of spontaneous activity of the whole brain—not simply the visual cortex—was one of the strengths of our research method. Also, through correlation with the retrievable clinical index, we investigated the possible underlying neurophysiological mechanism of PACG. Moreover, in combination with previous findings of our team, by using different analytical methods of resting-state fMRI, we expect to offer new ideas, and potentially generate a new avenue of future research in PACG.

There are several limitations to our study. First of all, the patients' emotion scales were not collected. PACG patients have been reported to be more sensitive to negative affective states, such as depression and anxiety, when compared to HCs or even POAG patients. Detailed mental scales should be taken into account in any related further study. Second, longitudinal research is lacking. The duration of disease varies greatly, so it is still unclear what the specific time relationship between brain activity alterations and disease stage is.

### Conclusions

In conclusion, PACG patients showed decreased short-range FCD mainly in the visual and visual-associated cortex, with the value being positively correlated with RNFLT value. Increased short-range FCD regions involved in the visual and non-visual cortex, along with the short-range FCD value, were negatively correlated with the value of A C/D. Additionally, we demonstrated that decreased long-range FCD was located in the non-visual cortex, which was functionally connected with the visual cortex.

### Acknowledgements

The authors would like to thank all the patients and volunteers in the study for their helpful participation.

*Funding:* This study was supported by the Natural Science Foundation of China (No:81760307).

### Footnote

*Conflicts of Interest:* The authors have no conflicts of interest to declare.

*Ethical Statement:* This study complied with the Declaration of Helsinki, and the Human Research Ethics Committee of the First Affiliated Hospital of Nanchang University approved the study protocol. Written informed consent was obtained from each participant prior to the study.

### References

1. Mantravadi AV, Vadhar N. Glaucoma. *Prim Care* 2015;42:437-49.
2. Davis BM, Crawley L, Pahlitzsch M, Javaid F, Cordeiro ME. Glaucoma: the retina and beyond. *Acta Neuropathol* 2016;132:807-26.
3. Ramirez AI, de Hoz R, Salobar-Garcia E, Salazar JJ, Rojas B, Ajoy D, López-Cuenca I, Rojas P, Triviño A, Ramírez JM. The Role of Microglia in Retinal Neurodegeneration: Alzheimer's Disease, Parkinson, and Glaucoma. *Front Aging Neurosci* 2017;9:214.
4. Ghiso JA, Doudevsk I, Ritch R, Rostagno AA. Alzheimer's Disease and Glaucoma: Mechanistic Similarities and Differences. *J Glaucoma* 2013;22 Suppl 5:S36-8.
5. Danesh-Meyer HV, Levin LA. Glaucoma as a neurodegenerative disease. *J Neuroophthalmol* 2015;35 Suppl 1:S22-8.
6. Li T, Liu Z, Li J, Liu Z, Tang Z, Xie X, Yang D, Wang N, Tian J, Xian J. Altered amplitude of low-frequency fluctuation in primary open-angle glaucoma: a resting-state FMRI study. *Invest Ophthalmol Vis Sci* 2014;56:322-9.
7. Song Y, Mu K, Wang J, Lin F, Chen Z, Yan X, Hao Y, Zhu W, Zhang H. Altered spontaneous brain activity in primary open angle glaucoma: a resting-state functional magnetic resonance imaging study. *PLoS One* 2014;9:e89493.
8. Frezzotti P, Giorgio A, Toto F, De Leucio A, De Stefano N. Early changes of brain connectivity in primary open angle glaucoma. *Hum Brain Mapp* 2016;37:4581-96.
9. Peng Zhou, Jieqiong Wang, Ting Li, Ningli Wang, Junfang Xian, Huiguang He. Abnormal interhemispheric resting-state functional connectivity in primary open-angle glaucoma. *Conf Proc IEEE Eng Med Biol Soc* 2016;2016:4055-58.
10. Li S, Li P, Gong H, Jiang F, Liu D, Cai F, Pei C, Zhou F, Zeng X. Intrinsic Functional Connectivity Alterations

- of the Primary Visual Cortex in Primary Angle-Closure Glaucoma Patients before and after Surgery: A Resting-State fMRI Study. *PLoS One* 2017;12:e0170598.
11. Cai F, Gao L, Gong H, Jiang F, Pei C. Network Centrality of Resting-State fMRI in Primary Angle-Closure Glaucoma Before and After Surgery. *PLoS One* 2015;10:e0141389.
  12. Huang X, Zhong YL, Zeng XJ, Zhou F, Liu XH, Hu PH, Pei CG, Shao Y, Dai XJ. Disturbed spontaneous brain activity pattern in patients with primary angle-closure glaucoma using amplitude of low-frequency fluctuation: a fMRI study. *Neuropsychiatr Dis Treat* 2015;11:1877-83.
  13. Tomasi D, Volkow ND. Aging and functional brain networks. *Mol Psychiatry* 2012;17:471, 549-58.
  14. Zang Y, Jiang T, Lu Y, He Y, Tian L. Regional homogeneity approach to fMRI data analysis. *Neuroimage* 2004;22:394-400.
  15. Biswal B, Yetkin FZ, Haughton VM, Hyde JS. Functional connectivity in the motor cortex of resting human brain using echo-planar MRI. *Magn Reson Med* 1995;34:537-41.
  16. Fox MD, Raichle ME. Spontaneous fluctuations in brain activity observed with functional magnetic resonance imaging. *Nat Rev Neurosci* 2007;8:700-11.
  17. Fransson P, Marrelec G. The precuneus/posterior cingulate cortex plays a pivotal role in the default mode network: Evidence from a partial correlation network analysis. *Neuroimage* 2008;42:1178-84.
  18. Tomasi D, Volkow ND. Functional connectivity density mapping. *Proc Natl Acad Sci U S A* 2010;107:9885-90.
  19. Tomasi D, Volkow ND. Association between functional connectivity hubs and brain networks. *Cereb Cortex* 2011;21:2003-13.
  20. He Y, Chen ZJ, Evans AC. Small-World Anatomical Networks in the Human Brain Revealed by Cortical Thickness from MRI. *Cereb Cortex* 2007;17:2407-19.
  21. Mégevand P, Groppe DM, Goldfinger MS, Hwang ST, Kingsley PB, Davidesco I, Mehta AD. Seeing Scenes: Topographic Visual Hallucinations Evoked by Direct Electrical Stimulation of the Parahippocampal Place Area. *J Neurosci* 2014;34:5399-405.
  22. Chen W, Zhang L, Xu Y, Zhu K, Luo M. Primary angle-closure glaucomas disturb regional spontaneous brain activity in the visual pathway: an fMRI study. *Neuropsychiatr Dis Treat* 2017;13:1409-17.
  23. Boucard CC, Hernowo AT, Maguire RP, Jansonius NM, Roerdink JB, Hooymans JM, Cornelissen FW. Changes in cortical grey matter density associated with long-standing retinal visual field defects. *Brain* 2009;132:1898-906.
  24. Yu L, Xie L, Dai C, Xie B, Liang M. Progressive thinning of visual cortex in primary open-angle glaucoma of varying severity. *PLoS One* 2015;10:e0121960.
  25. Chan KC, So K, Wu EX. Proton magnetic resonance spectroscopy revealed choline reduction in the visual cortex in an experimental model of chronic glaucoma. *Exp Eye Res* 2009;88:65-70.
  26. Lester BD, Dassonville P. The Role of the Right Superior Parietal Lobule in Processing Visual Context for the Establishment of the Egocentric Reference Frame. *J Cogn Neurosci* 2014;26:2201-09.
  27. Wang K, Jiang T, Yu C, Tian L, Li J, Liu Y, Zhou Y, Xu L, Song M, Li K. Spontaneous activity associated with primary visual cortex: a resting-state FMRI study. *Cereb Cortex* 2008;18:697-704.
  28. Dai H, Morelli JN, Ai F, Yin D, Hu C, Xu D, Li Y. Resting-state functional MRI: functional connectivity analysis of the visual cortex in primary open-angle glaucoma patients. *Hum Brain Mapp* 2013;34:2455-63.
  29. Zhang J, Bi W, Zhang Y, Zhu M, Zhang Y, Feng H, Wang J, Zhang Y, Jiang T. Abnormal functional connectivity density in Parkinson's disease. *Behav Brain Res* 2015;280:113-8.
  30. Scheff SW, Price DA, Schmitt FA, Roberts KN, Ikonovic MD, Mufson EJ. Synapse Stability in the Precuneus Early in the Progression of Alzheimer's Disease. *J Alzheimers Dis* 2013;35:599-609.
  31. Wang T, Li Q, Guo M, Peng Y, Li Q. Abnormal functional connectivity density in children with anisometropic amblyopia at resting-state. *Brain Res* 2014;1563:41-51.
  32. Chen WW, Wang N, Cai S, Fang Z, Yu M, Wu Q, Tang L, Guo B, Feng Y, Jonas JB, Chen X, Liu X, Gong Q. Structural brain abnormalities in patients with primary open-angle glaucoma: a study with 3T MR imaging. *Invest Ophthalmol Vis Sci* 2013;54:545-54.
  33. Catani M, Jones DK, Donato R, Ffytche DH. Occipito-temporal connections in the human brain. *Brain* 2003;126:2093-107.
  34. O'Hare F, Rance G, Crowston JG, McKendrick AM. Auditory and Visual Temporal Processing Disruption in Open Angle Glaucoma. *Invest Ophthalmol Vis Sci* 2012;53:6512-18.
  35. Putcha D, Ross RS, Cronin-Golomb A, Janes AC, Stern CE. Salience and Default Mode Network Coupling Predicts Cognition in Aging and Parkinson's Disease. *J Int Neuropsychol Soc* 2016;22:205-15.

36. Yuan C, Zhu H, Ren Z, Yuan M, Gao M, Zhang Y, Li Y, Meng Y, Gong Q, Lui S, Qiu C, Zhang W. Precuneus-related regional and network functional deficits in social anxiety disorder: A resting-state functional MRI study. *Compr Psychiatry* 2018;82:22-29.
37. Kandilarova S, Stoyanov D, Kostianev S, Specht K. Altered Resting State Effective Connectivity of Anterior Insula in Depression. *Front Psychiatry* 2018;9:83.
38. Zhang X, Olson DJ, Le P, Lin FC, Fleischman D, Davis RM. The Association Between Glaucoma, Anxiety, and Depression in a Large Population. *Am J Ophthalmol* 2017;183:37-41.
39. Agorastos A, Skevas C, Matthaei M, Otte C, Klemm M, Richard G, Huber CG. Depression, Anxiety, and Disturbed Sleep in Glaucoma. *J Neuropsychiatry Clin Neurosci* 2013;25:205-13.
40. Kashiwagi K, Okubo T, Tsukahara S. Association of Magnetic Resonance Imaging of Anterior Optic Pathway with Glaucomatous Visual Field Damage and Optic Disc Cupping. *J Glaucoma* 2004;13:189-95.
41. Hales JB, Brewer JB. Parietal and frontal contributions to episodic encoding of location. *Behav Brain Res* 2013;243:16-20.
42. Yang YL, Deng HX, Xing GY, Xia XL, Li HF. Brain functional network connectivity based on a visual task: visual information processing-related brain regions are significantly activated in the task state. *Neural Regen Res* 2015;10:298-307.

**Cite this article as:** Chen L, Li S, Cai F, Wu L, Gong H, Pei C, Zhou F, Zeng X. Altered functional connectivity density in primary angle-closure glaucoma patients at resting-state. *Quant Imaging Med Surg* 2019;9(4):603-614. doi: 10.21037/qims.2019.04.13